ISSN 1024-8560, Atmospheric and Oceanic Optics, 2014, Vol. 27, No. 2, pp. 123–129. © Pleiades Publishing, Ltd., 2014.
Original Russian Text © V.V. Kolosov, V.V. Dudorov, G.A. Filimonov, A.S. Panina, M.A. Vorontsov, 2013, published in Optica Atmosfery i Okeana.

OPTICAL WAVES PROPAGATION

# Accounting for the Effect of Large-Scale Atmospheric Inhomogeneities in Problems of Laser Radiation Propagation along Long High-Altitude Paths

**V. V. Kolosov[a], V. V. Dudorov[a], G. A. Filimonov[a], A. S. Panina[a], and M. A. Vorontsov[b]**

[a] *V.E. Zuev Institute of Atmospheric Optics, Siberian Branch, Russian Academy of Sciences, pl. Akademika Zueva 1, Tomsk, 634021 Russia*
*e-mail: dvv@iao.ru*

[b] *University of Dayton, 300 College Park, Dayton, OH 45469, USA*

Received August 20, 2012

**Abstract**—We show that large-scale atmospheric inhomogeneities observed experimentally can significantly affect optical radiation propagation along long paths, and it is impossible to take into account this effect within the classical turbulence model. We suggest a new algorithm for numerical simulation of laser beam propagation along long low-inclined atmospheric paths with large-scale atmospheric inhomogeneities, which allows one to consider beam refraction and focusing at large-scale inhomogeneities along with beam distortions due to small-scale inhomogeneities and regular refraction in a vertical plane.

**DOI:** 10.1134/S1024856014020092

## INTRODUCTION

Growing interest in the design of optical systems capable of operating efficiently at long distances (>100 km) in the atmosphere under different conditions is caused by the rapid development of wireless optical communications, remote sensing, active and passive target observation, tracking, and recognition, and problems of optical energy transfer to remote objects. When optical waves propagate in the atmosphere to long distances, turbulent distortions can cause significant variations in the parameters of a wave received and thus strongly affect the operational efficiency of optical systems.

The turbulence effect during laser radiation propagation along atmospheric paths is usually connected with radiation intensity fluctuations, beam wandering and broadening, spatially inhomogeneous distortions of images, generation of singularities (branch points) of the wave phase front, and so on [1–4].

At present, the analysis of atmospheric turbulence effects is based on theoretical and numerical models derived from classical Kolmogorov–Obukhov turbulence theory [5–8]. It was developed in the 1940–1960s and repeatedly confirmed by different atmospheric experiments. Most of these experiments were carried out along relatively short atmospheric paths (no longer than several tens of kilometers [9–12]).

In the past decade, more and more researchers concluded that extension of the classical Kolmogorov–Obukhov turbulence theory to the analysis of the atmospheric turbulence effect on long-distance optical wave propagation is ungrounded. Many quite long-path experiments [13–19] point to significant deviations of the results from this model.

One of the reasons for this deviation can be neglect of large-scale atmospheric inhomogeneities (comparable with the radiation propagation distance) within the classical model. Occurrence of these inhomogeneities is caused by the dynamics of large-scale air flows that lead to the formation of inhomogeneous atmospheric layers with a large variety of self-organizing spatiotemporal coherent structures, including gravity waves, Benard cells, jets and stratified flows, and other atmospheric instabilities, which result in nonstationary refractive effects.

In this work, we show that large-scale atmospheric inhomogeneities observed experimentally can strongly affect radiation propagation. In addition, we show that accounting for this effect within the classical turbulence model is impossible.

## CHARACTERISTICS OF MODEL AND MEASURED INHOMOGENEITIES OF ATMOSPHERIC REFRACTIVE INDEX

Let us consider laser radiation propagation along low-inclined high-altitude (10–30 km) paths 100–500 km long. A common approach to solution of the problem of optical radiation propagation in an inhomogeneous atmosphere reduces to accounting for two factors: turbulence (beam distortion on random inhomogeneities) and regular refraction (beam shift as a whole). Such problems are usually studied by numerical methods, within which the turbulence is simulated by a sequence of phase screens. The variance of screen

phase fluctuations is determined by the values of the structure parameter of refractive index $C_n^2$ at altitudes specified. In this case, limitation of the lateral size of the phase screens set on a finite computational grid correspondingly limits the size of atmospheric inhomogeneities (to several tens of meters) which are considered in simulation by common methods. As is shown below, the use of turbulent screens with an outer scale larger than the screen size [21–23] does not allow the effect of large-scale inhomogeneities occurring in the real atmosphere to be considered as well. For scales much larger than the beam cross-section size, only an averaged variation in the air density with altitude is considered. It is supposed that this air density inhomogeneity results in regular radiation diffraction (vertical beam shift) without other beam distortions.

To calculate the regular diffraction, different models of vertical air density distribution can be used [24, 25]. The International Standard Atmosphere (ISA) is used quite often, i.e., a hypothetical vertical air density distribution throughout the Earth's atmosphere, which, according to an international agreement, represents the annual average and midlatitude state [26].

The air density profile is not a linear function of altitude in ISA. That is, in addition to a nonzero gradient of the refractive index, it provides nonzero second derivatives of the refractive index. Hence, there is not only linear inhomogeneity of the refractive index within a beam cross-section, but also quadratic inhomogeneity that causes radiation focusing or defocusing.

The refraction length $L_R$ is used in nonlinear optics to describe the focusing (defocusing) effect of an inhomogeneous medium (by analogy with the diffraction length). The refraction length determines the distance at which the quadratic inhomogeneity of the refractive index causes noticeable beam focusing or defocusing. This length is connected with the second derivative of the refractive index $n_2 = d^2n/dR^2$ by the following equation:

$$L_R = \frac{1}{\sqrt{\left|\frac{d^2n}{dR^2}\right|}} = \frac{1}{n_2^{1/2}}, \qquad (1)$$

where $R$ is the coordinate in a plane normal to the beam propagation axis.

Calculation of the refraction length for the air density distribution corresponding to ISA at different altitudes (see below, minus means focusing) was carried out with the use of the following relationship between perturbations of the refractive index $n'$ and air density $\rho'$: $n' = G\rho'$, where $G$ is the Gladstone–Dale constant. This constant is $0.226 \times 10^{-3}$ m$^3$/kg for light with the wavelength $\lambda = 632.8$ nm for air temperature of 288 K and pressure of 0.1013 MPa.

| $H$, m | $L_R$, km |
|---|---|
| 3000 | 780.6 |
| 10000 | 964.3 |
| 11000 | −559.1 |
| 12000 | 763.9 |
| 15000 | 968.3 |
| 20000 | 1379.6 |
| 25000 | 2094.5 |

It is seen that a focusing channel with a characteristic refraction length (focusing length) of 559.1 km is formed at an altitude of 11 km. That is, the refraction length becomes comparable with the propagation distance even for a maximally smoothed model of vertical density distribution. When using other density distribution models, e.g., the summer or winter midlatitude model, the refraction length becomes even smaller.

Let us note that the model air density distributions used are inhomogeneous only in the vertical direction, while they do not manifest in variations in the horizontal beam size. However, it is evident that the real state of the atmosphere always deviates from model states. Occurrence of random deviations from the smoothed profile results in an additional increase in the modulus of the second derivative of the refractive index with respect to the vertical coordinate and a nonzero second derivative with respect to the horizontal coordinate (decrease in the refraction length).

In the real anisotropic atmosphere, mean values of the second derivatives of the refractive index differ in vertical and horizontal directions [16]. However, assuming that both components of the second derivative of the refractive index are of one order, we estimate the radiation refraction length in the real atmosphere on the basis of vertical air density distributions measured [27, 28]. These measurements have been carried out for altitudes higher than 20 km. Based on Eq. (1), we can find that the refraction length is about 300–600 km at altitudes of 20–24 km. If we assume that relative density deviations from ISA have the same character at other altitudes, then we can find that $L_R \approx$ 150–350 km at an altitude of 10 km and 100–250 km at an altitude of 3 km.

The relative perturbation of air density relative to ISA in the lidar data [27, 28] is measured with an altitude resolution of 192 m, i.e., it characterizes atmospheric inhomogeneities with scales larger than 200 m. The characteristic vertical sizes of air density inhomogeneities are 1–2 km in this case. Vertical density profiles have been measured at 10-minute intervals. By analogy with the frozen turbulence hypothesis [29], these measurements can be extended in space along the wind velocity vector, and the horizontal sizes of

inhomogeneities, which vary in this case within wide limits from 10 to 60 km, can be estimated.

## ESTIMATION OF THE EFFECT OF LARGE-SCALE INHOMOGENEITIES ON RADIATION PROPAGATION WITHIN THE KOLMOGOROV–OBUKHOV MODEL

Let us estimate the effect of large-scale atmospheric inhomogeneities on laser radiation propagation along long paths. First, we estimate the effect within the classical Kolmogorov–Obukhov model for homogeneous (quasi-homogeneous) and isotropic turbulence. For this, we use the approach suggested in [1], within which turbulent inhomogeneities are represented by lenses bounded by spherical surfaces. This qualitative approach allowed the authors [1] to derive an equation for amplitude and wave phase fluctuations, which coincide with results of the method of smooth perturbations (MSP) accurate to numerical coefficients.

Let $l_n$ be the diameter of a spherical lens and $n_{li}$ be the deviation of the refractive index inside the $i$th lens from the medium average value. Then the focal length of this lens $F_i = l_n/2n_{li}$. $N = L/l_n$ inhomogeneities fall on a propagation path of length $L$. The total optical power $1/F_\Sigma$ of several weak lenses, distances between which are small in comparison with their focal lengths, is equal to a sum of optical powers of individual lenses, i.e.,

$$1/F_\Sigma = \sum_{i=1}^{N} 1/F_i = \sum_{i=1}^{N} 2n_{li}/l_n. \qquad (2)$$

Supposing statistical independence of perturbations of the refractive index in the lenses, the variance of the total optical power of inhomogeneities along the path is defined as

$$\left\langle (1/F_\Sigma)^2 \right\rangle = \frac{4\langle n_l^2 \rangle}{l_n^2} N = \frac{4\langle n_l^2 \rangle L}{l_n^3}, \qquad (3)$$

where angular brackets mean averaging over realizations of random inhomogeneities.

The structure function of the refractive index in the following form answers to the classical turbulence model:

$$D_n(\rho) = C_n^2 \rho^{2/3}. \qquad (4)$$

Again, an inhomogeneity of $l_n$ in size is characterized by fluctuations of the refractive index of about

$$\langle n_l^2 \rangle^{1/2} = C_n l_n^{1/3}. \qquad (5)$$

Substituting Eq. (5) in Eq. (3), we find

$$\left\langle (1/F_\Sigma)^2 \right\rangle = \frac{4C_n^2 L}{l_n^{7/3}}.$$

Correspondingly, the standard deviation of the total focal length along the path caused by inhomogeneities of $l_n$ in size can be estimated as

$$\sigma_{F_\Sigma} \cong \frac{l_n^{7/6}}{2C_n L^{1/2}}. \qquad (6)$$

Equation (6) allows effects of inhomogeneities of different sizes to be estimated. Below we represent the estimation results of the standard deviation of the total focal length for the distance $L = 500$ km and $C_n^2 = 10–15$ m$^{-2/3}$; this value, according to the Gurvich models [30], is maximal for an altitude of 20 km:

| $l_n$, m | $\sigma_{F_\Sigma}$, km |
|---|---|
| 0.1 | 1.5 |
| 1.0 | 22.4 |
| 10.0 | 328.2 |
| 20.0 | 736.8 |
| 50.0 | 2145.9 |
| 100.0 | 4817.5 |

It is seen that optical effect of the inhomogeneities on radiation rapidly weakens as their size increases. The focusing effect of inhomogeneities of about 100 m in size and larger manifests at distances several-fold longer that the propagation distance and, hence, this effect can be neglected. We should note that this conclusion is valid for results obtained on the basis of Eq. (6) for the classical turbulence.

## ESTIMATION OF THE EFFECT OF EXPERIMENTALLY RECORDED LARGE-SCALE ATMOSPHERIC INHOMOGENEITIES ON RADIATION PROPAGATION

Let us now estimate inhomogeneities recorded in the lidar experiments [27, 28] in a similar way. Let an inhomogeneity be characterized by the second derivative of the refractive index $n_2$ and have the length $l_z$ along a propagation path. In this case, the focal length of the $i$th inhomogeneity $F_i = 1/l_z n_{2i}$. $N = L/l_z$ inhomogeneities fall on the propagation path of $L$ in length, and their total optical power

$$1/F_\Sigma = \sum_{i=1}^{N} 1/F_i = \sum_{i=1}^{N} l_z n_{2i}.$$

Supposing, as above, statistical independence of perturbations of the refractive index in the inhomogeneities, the variance of the total optical power of the inhomogeneities along the path is

$$\left\langle (1/F_\Sigma)^2 \right\rangle = \left\langle \left( \sum_{i=1}^{N} l_z n_{2i} \right)^2 \right\rangle = N l_z^2 \left\langle n_2^2 \right\rangle = L l_z \left\langle n_2^2 \right\rangle.$$

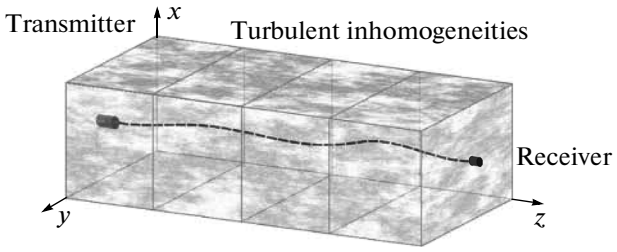


**Fig. 1.** 3D refractive index distribution.

Correspondingly, the estimate of the standard deviation of the total focal length along the path with inhomogeneities of $l_z$ in size can be written as

$$\sigma_{F_\Sigma} \cong 1\Big/\left(Ll_z\left\langle n_2^2\right\rangle\right)^{1/2} = L_R^2\Big/(Ll_z)^{1/2}, \qquad (7)$$

where $L_R$ is the refraction length connected with perturbations of the refractive index by Eq. (1).

As is shown above, the second derivatives of the refractive index give the refraction length of about 300–600 km at altitudes of 20–24 km. Let $L_R$ = 400 km, then we find the following values of the standard deviation of the total focal length depending on the longitudinal size of inhomogeneities for the distance $L$ = 500 km:

| $l_z$, km | $\sigma_{F_\Sigma}$, km |
|---|---|
| 5 | 4131.2 |
| 10 | 2262.7 |
| 20 | 1600.0 |
| 50 | 1011.9 |
| 100 | 715.5 |

It is seen that the effect of the inhomogeneities on beam propagation becomes stronger with an increase in the inhomogeneity sizes in this case, in contrast to the classical turbulence model.

The above estimates are rough, but they allow us to consider the role of large-scale inhomogeneities within one approach and draw the following conclusion. Large-scale inhomogeneities observed experimentally [27, 28] should be taken into account during simulation of laser radiation propagation along long paths, but this is impossible within the classical turbulence model.

Thus, a need in a new atmospheric turbulence model arises for the problem of numerical simulation of laser radiation propagation along long atmospheric paths.

## TURBULENT ATMOSPHERIC MODEL CONSIDERING LARGE-SCALE INHOMOGENEITIES

Adaptation of the classical method based on the formation of turbulent phase screens to simulation of large-scale atmospheric inhomogeneities meets two difficulties. First, it is difficult to satisfy the condition of statistical independence for these screens; for this, they should be distanced too far from each other, farther than the inhomogeneity size. Second, construction of these screens is based on a known spectrum of phase fluctuations of a plane wave in a turbulent medium. However, these spectra have been built only for the classical turbulence and, as is shown above, cannot be generalized to large-scale inhomogeneities. The use of turbulence spectra different from the Kolmogorov spectrum [31, 32] does not allow correct accounting for the effect of inhomogeneities about 1 km in size present in the real atmosphere as well.

Therefore, a model that includes large-scale inhomogeneities should be based on a 3D air density (refractive index) distribution. This distribution can be a result of both in situ measurements (ground-based, airborne, satellite, etc.) and numerical simulation of atmospheric currents. This distribution of the refractive index is representable as a 3D data array (Fig. 1) in simulation problems.

The estimates of the effect of large-scale inhomogeneities given in this work allow a conclusion that an optimal step for the computational grid in a plane normal to the radiation propagation axis is about 100 m. In this case, smaller inhomogeneities can be taken into account with the use of classical 2D phase screens, and a 3D refractive index distribution measured (or simulated) can be used for larger inhomogeneities.

The lidar measurement results of large-scale atmospheric inhomogeneities [27, 28] allow construction of a (zero) 3D turbulence model. By analogy with the frozen turbulence, we can extend these measurements (vertical air density distributions) in a horizontal direction along the wind velocity vector and find a spatial distribution of the inhomogeneities in the *XOZ* plane (if the wind velocity vector is codirectional with the propagation axis *OZ*).

To construct the 3D distribution, we should make some assumptions about measurement of air density in a horizontal direction normal to the wind. We can assume that the air density changes in this direction similar to the density change in a direction along the wind velocity vector or in a vertical direction. The transverse dimensions of the resulting 3D array can be several kilometers or more. In our case (on the basis of measurements [27, 28]), the 3D distribution of the refractive index is to be constructed with a lateral step of 192 m along the vertical axis *OX*.

The construction of the 3D array allows us to proceed to the next step—the calculation of the beam refraction (beam shift as a whole). This refraction con-

sists of the regular refraction in a vertical plane at the mean air density profile (ISA or other atmospheric model chosen) and the refraction in vertical and horizontal planes at large-scale inhomogeneities on the basis of the resulting (measured or simulated) 3D data array (see Fig. 1). There are many methods for calculation of the regular refraction. A parabolic equation (i.e., paraxial approximation) is usually used in the calculation of radiation propagation; therefore, we calculate the regular refraction in this approximation. Geometrical beam bending (refraction) in the paraxial approximation is defined by the equation

$$\frac{d^2\mathbf{R}}{dz^2} = \nabla_{\mathbf{R}} n(z, \mathbf{R}), \tag{8}$$

where $\mathbf{R} = \{x, y\}$ is the radius-vector in a plane normal to the propagation axis $OZ$.

Refractive index gradient (8) is connected with the vertical air density profile via the following equation:

$$\nabla_{\mathbf{R}} n(z, \mathbf{R}) = \frac{dn}{d\rho} \nabla_{\mathbf{R}} \rho(z, \mathbf{R}), \tag{9}$$

where $\frac{dn}{d\rho} = G$ is the Gladstone–Dale constant.

Solving Eq. (8) for the axial ray of a laser beam (using interpolation in the calculation of gradients at internode points of the 3D array) we plot a trajectory of the axial ray (dashed curve in Fig. 1). The refractive index gradient is constant on the scale of laser beam transverse dimension (1–2 m) for inhomogeneities larger than 200 m; therefore, all other rays of this beam shift parallel to the axial ray. For further calculations, we change coordinates to a new system where the longitudinal axis coincides with the ray trajectory calculated for the axial beam (dashed curve in Fig. 1).

When solving the long-path propagation problem, we should take into account inhomogeneities on all scales. Therefore, after calculation of the regular diffraction, we supplement the 3D turbulence model (data array) with a set of classical phase screens that simulate inhomogeneities smaller than 100 m. As a result, we obtained a turbulence model in the form shown in Fig. 2.

The axis of this figure coincides with the ray trajectory (dashed curve); it is straight in these coordinates. Transverse sizes in this figure are chosen, as is usual in similar calculations, i.e., several maximal (along the propagation path) laser beam sizes. The phase screens simulate inhomogeneities from 1 cm to tens of meters. The medium between the screens simulates large-scale inhomogeneities obtained from experimental data or from numerical simulation of atmospheric currents 100 m in size and larger. Thus, the atmospheric model shown in Fig. 2 covers the whole spectrum of atmospheric inhomogeneities.

It is evident that not only the gradient of refractive index inhomogeneity is constant within the transverse

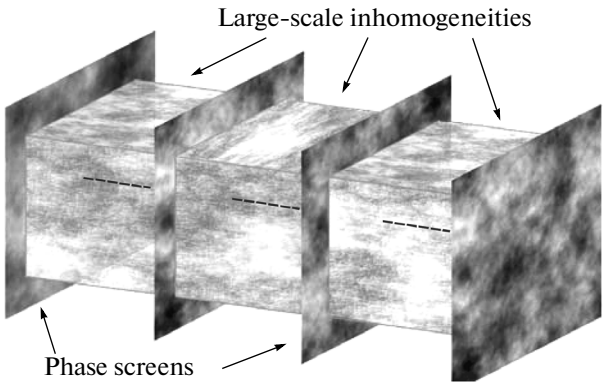


**Fig. 2.** 3D model of turbulent medium.

beam size (1–2 m), but also its second derivatives. Then, the distribution of refractive index perturbations between the turbulent screens in Fig. 2 can be represented as

$$\Delta n(z, x, y) = \frac{d^2 n(z, x, y)}{dx^2} x^2 + \frac{d^2 n(z, x, y)}{dy^2} y^2 \equiv n_{xx}(z)x^2 + n_{yy}(z)y^2, \tag{10}$$

where the second derivatives, as the gradients, are calculated at a point on the axial ray (dashed curve in Fig. 1) by the interpolation method. There are no gradients (first derivatives) in expansion (10), since their effect on the radiation propagation was considered at the previous step, when solving Eq. (8).

Hence, simulation of laser radiation propagation along a long path reduces to the numerical solution of the parabolic equation for a medium represented by the 3D turbulence model (see Fig. 2). This approach differs from the classical method in the presence of refraction medium (10) between turbulent screens. Therefore, the problem of radiation propagation between the screens cannot be solved like the diffraction problem, since it requires additional construction of refraction screens. Dividing the distance between the screens to steps $\Delta z$, we form a phase screen in each plane $z_i$ with a parabolic phase distribution of $S(z_i, x, y)$, corresponding to the geometrical phase incursion during a step (10):

$$S(z_i, x, y) = k\Delta z n(z_i, x, y) = \frac{1}{2} k\Delta z (n_{xx}(z)x^2 + n_{yy}(z)y^2). \tag{11}$$

Thus arranging turbulent and refraction screens along the path, we calculate the laser radiation propagation by a common scheme.

The above algorithm for numerical simulation of laser beam propagation along slightly inclined atmospheric paths is actually a development of the traditional half-split method to the case of joint accounting

for turbulence and refraction at large-scale inhomogeneities. The algorithm consists of three steps. First, it is necessary to built a 3D array that simulates large-scale (100 m and larger) inhomogeneities of distribution of the refractive index of an inhomogeneous medium (atmosphere). During the next step, the geometrical trajectory of the axial beam is calculated in this medium. Simultaneously, the first and second lateral derivatives of the refractive index are calculated to construct the 3D turbulence model (see Fig. 2). During the last step, the parabolic equation is solved for the turbulent medium with regular inhomogeneities of the refractive index.

## CONCLUSIONS

The approach to the problem of propagation simulation presented in this work differs significantly from the classical approach. Within the model suggested, beam refraction and focusing at large-scale inhomogeneities can be taken into account along with beam distortions at small-scale inhomogeneities and its regular vertical refraction. In the next work, we will show that the presence of large-scale inhomogeneities similar to those observed in the experiment [27, 28] can strongly affect the radiation propagation and, in particular, significantly change the diffraction limit for a long propagation path. This change can be toward both increase and decrease in the diffraction limit depending on implementation of large-scale density fluctuations along the path.

We will also show that methods developed in the theory of aberration-free Gaussian beam propagation allow a significant increase in the speed of numerical calculations during solution of the parabolic equation for the given turbulence model without loss of accuracy.

## ACKNOWLEDGMENTS

The authors are grateful to V. N. Marichev for the initial lidar data on air density [27, 28]. The work was supported by the Ministry of Science and Education of the Russian Federation (agreement no. 8510).

## REFERENCES

1. S. M. Rytov, Yu. A. Kravtsov, and V. I. Tatarskii, *Introduction to Statistical Radiophysics. Random Fields* (Nauka, Moscow, 1978) [in Russian].
2. V. E. Zuev, *Propagation of Visible and IR Waves in the Atmosphere* (Sov. radio, Moscow, 1970) [in Russian].
3. A. Ishimaru, *Wave Propagation and Scattering in Random Media* (Academic Press, New York, 1978).
4. D. L. Fried and J. L. Vaughn, "Branch cuts in the phase function," Appl. Opt. **31** (15), 2865–2882 (1992).
5. A. N. Kolmogorov, "The local structure of turbulence in incompressible viscous fluid for very large Reynolds numbers," Dokl. Akad. Nauk SSSR **30** (4), 299–303 (1941).
6. A. M. Obukhov, "On the distribution of energy in the spectrum of turbulent flow," Dokl. Akad. Nauk SSSR **32** (1), 22–24 (1941).
7. V. I. Tatarskii, *Wave Propagation in a Turbulent Medium* (McGraw-Hill, New York, 1961).
8. V. I. Tatarskii, *The Effects of the Turbulence Atmosphere on Wave Propagation* (Keter Press, Jerusalem, 1971).
9. M. E. Gracheva and A. S. Gurvich, "Strong fluctuations in the intensity of light propagated through the atmosphere close to the Earth," Izv. Vyssh. Uchebn. Zaved. Radiofiz. **8** (4), 711–724 (1965).
10. W. A. Coles and R. G. Frehlich, "Simultaneous measurements of angular scattering and intensity scintillation in the atmosphere," J. Opt. Soc. Amer. **72** (8), 1042–1048 (1982).
11. R. L. Phillips and L. C. Andrews, "Measured statistics of laser-light scattering in atmospheric turbulence," J. Opt. Soc. Amer. **71** (12), 1440–1445 (1981).
12. A. Consortini, F. Cochetti, J. H. Churnside, and R. J. Hill, "Inner-scale effect on irradiance variance measured for weak-to-strong atmospheric scintillation," J. Opt. Soc. Amer., A **10** (11), 2354–2362 (1993).
13. W. A. Bernard, B. M. Welsh, M. C. Roggemann, and R. J. Feldmann, "Atmospheric turbulence characterization of a low-altitude long horizontal path," Proc. SPIE **2828**, 198–209 (1996).
14. N. Perlot, D. Giggenbach, H. Henniger, J. Horwath, M. Knapek, and K. Zettl, "Measurements of the beam wave fluctuations over a 142 km atmospheric path," Proc. SPIE **6304**, 63041O (2006).
15. W. M. Hughes and R. B. Holmes, "Pupil-plane imager for scintillometry over long horizontal paths," Appl. Opt. **46** (29), 7099–7109 (2007).
16. M. S. Belen'kii, E. Cuellar, K. A. Hughes, and V. A. Rye, "Preliminary experimental evidence of anisotropy of turbulence at Maui Space Surveillance Site," in *Proc. of AMOS Conf.*, Ed. by S. Ryan (2006), pp. 538–547.
17. G. R. Ochs, R. R. Bergman, and J. R. Snyder, "Laser beam scintillation over horizontal paths from 5.5 to 145 kilometers," J. Opt. Soc. Amer. **59**, 231–234 (1969).
18. M. A. Vorontsov, G. W. Carhart, V. S. Rao Gudimetla, T. Weyrauch, E. Stevenson, S. L. Lachinova, L. A. Beresnev, J. Liu, K. Rehder, and J. F. Riker, "Characterization of atmospheric turbulence effects over 149 km propagation path using multi-wavelength laser beacons," in *Proc. Advanced Maui Optical and Space Surveillance Technologies Conference*, *Maui, Hawaii, September 14–17, 2010*, Ed. by S. Ryan (The Maui Economic Development Board), p. E18.
19. M. Vorontsov, J. Riker, G. Carhart, V. S. Gudimetla, L. Beresnev, T. Weyrauch, and L. Roberts, "Deep turbulence effects compensation experiments with a cascaded adaptive optics system using a 3.63 m telescope," Appl. Opt. **48** (1), 47–57 (2009).
20. A. S. Gurvich, M. E. Gorbunov, O. V. Fedorova, G. Kirchengast, V. Proschek, Abad G. González, and K. A. Tereszchuk, "Spatiotemporal structure of a laser beam over 144 km in a Canary Islands experiment," Apl. Opt. **51** (30), 7374–7383 (2012).

21. R. G. Lane, A. Glindemann, and J. C. Dainty, "Simulation of a Kolmogorov phase screen," Waves in Random Media **2** (3), 209–224 (1992).
22. V. A. Banakh, I. N. Smalikho, and A. V. Falits, "Effectiveness of the subharmonic method in problems of computer simulation of laser beam propagation in a turbulent atmosphere," Atmos. Ocean. Opt. **25** (2), 106–109 (2012).
23. A. M. Vorontsov and P. V. Paramonov, "Simulation of extended phase screens in problems of optical wave propagation through the atmosphere," Radiophys. Quant. Electron. **49** (1), 18–30 (2006).
24. M. A. Kolosov and A. V. Shabel'nikov, *Electromagnetic Wave Refraction in the Earth's Atmosphere* (Sov. radio, Moscow, 1976) [in Russian].
25. V. V. Vinogradov, *Atmospheric Effect on Geodetic Measurements* (Nedra, Moscow, 1992) [in Russian].
26. http://dic.academic.ru/dic.nsf/enc_tech/2697
27. V. N. Marichev and D. A. Bochkovskii, "Lidar measurements of air density in the middle atmosphere. Part 1. Modeling of the potential capabilities in the visible spectral range," Opt. Atmosf. Okeana **26** (7), 553–563 (2013).
28. V. N. Marichev and D. A. Bochkovskii, "Lidar measurements of air density in the middle atmosphere. Part 2. Modeling of the potential sounding capabilities in the UV spectrum," Opt. Atmos. Okeana **26** (8), 701–704 (2013).
29. G. I. Taylor, "The spectrum of turbulence," Proc. Roy Soc. Lond. **164**, 476–490 (1938).
30. A. S. Gurvich and M. E. Gracheva, "A simple model for calculation of turbulent noises in optics systems," Izv. AN SSSR, Fiz. Atmosf. Okeana **16** (10), 1107–1111 (1980).
31. A. S. Gurvich, V. V. Vorob'ev, and O. V. Fedorova, "Strong scintillation spectra behind the atmosphere with large- and small-scale inhomogeneities," Atmos. Ocean. Opt. **24** (4), 347–357 (2011).
32. V. V. Nosov, P. G. Kovaldo, V. P. Lukin, and A. V. Torgaev, "Atmospheric coherent turbulence," Atmos. Ocean. Opt. **26** (3), 201–206 (2013).

*Translated by O. Ponomareva*